Seabed image acquisition and survey design for cold water coral mound characterisation

Aaron Lim[1), 3)], *Adam Kane* [1)], *Aurélien Arnaubec* [2)] *and Andrew J. Wheeler* [1), 3)]

[1)] *School of Biological, Earth and Environmental Sciences, University College Cork, Distillery Fields, North Mall, Cork, Ireland*

[2)]*Unité Systèmes sous-Marins, Centre de Méditerranée, Ifremer, Zone Portuaire de Brégaillon, CS 20330, 83507 La Seyne/Mer Cedex, France*

[3)] *Irish Centre for Research in Applied Geosciences, University College Cork, Ireland*

*Corresponding author: aaron.lim@ucc.ie

Keywords: cold water corals, mounds, video survey design, sediments, habitat mapping

Abstract

Cold-water coral (CWC) habitats are commonly regarded as hotspots of biodiversity in the deep-sea. However, a standardised approach to monitoring the effects of climate change, anthropogenic impact and natural variability through video-surveying on these habitats is poorly-established. This study is the first attempt at standardising a cost-effective video-survey design specific to small CWC mounds in order to accurately determine the proportion of facies across their surface. The Piddington Mound of the Moira Mounds, Porcupine Seabight, offshore Ireland has been entirely imaged by downward-facing video in 2011 and 2015. The 2011 video data is navigated into a full-mound, georeferenced video mosaic. A quadrat-based manual classification of this video mosaic at 0.25 m^2 resolution shows the exact proportion of facies abundance across the mound surface. The minimum number of random downward-facing images from the mound are determined to accurately characterise mound surface facies proportions. This minimum sample size is used to test the effectiveness of various common

survey designs for ROV-video-based habitat investigations. Single-pass video lines are not representative of the mound surface whilst gridded survey designs yield best results, similar to 100% mound coverage. The minimum sample size and manual classification are applied to the 2015 video data to show a 19% mound surface facies change over 4 years at 0.25 m^2 resolution. The proportion of live coral facies show little change while coral rubble facies show most change. This highlights an inconsistency between temporally-separated data sets and implies that in 20 years, the mound surface may almost entirely change.

1 Introduction

Cold-water corals (CWC) are sessile, filter-feeding organisms found in many parts of the world's oceans, being common and well-studied in the NE Atlantic (Freiwald, 2002; Roberts et al., 2003; Roberts et al., 2006; Wheeler et al., 2007). Also referred to as "deep-water" corals, their distribution actually covers a large depth range being found from 39 m to 2000 m water depth (Freiwald et al., 2004; Roberts et al., 2006). As their name suggests, they typically exist in cooler waters from 4°C to 13°C (Freiwald, 2002) with the exception of *Oculina* spp., and within a salinity range of 31.7 ‰ - 38.8 ‰ (Davies et al., 2008). *Lophelia pertusa* is the most well-studied framework-forming CWC and is reliant on currents for food supply (Orejas et al., 2016; Purser et al., 2010 and references therein) and can form 3D carbonate structures that benefit from its ability to baffle currents and thereby enhance sedimentation (Wheeler, Kozachenko, et al., 2005; Wheeler et al., 2008). The complex hydrodynamic relationship between the CWC framework, food supply, currents and sedimentation often results in the generation of positive bathymetric features on the seabed called CWC mounds (De Mol et al., 2007; Dorschel, 2003; Squires, 1964; Wilson, 1979). Wilson (1979) and Squires (1964) describe the early-stage development of cold-water coral mounds using evidence from rock outcrop, museum specimens and submersible dives. Through successive and continuous

periods of CWC mound development in the same location, they can generate bathymetric features up to 350 m from base to summit (Henriet et al., 2014 and references therein). Evidence from a number of studies show that the continued development of these coral mounds is largely controlled by environmental conditions (Dullo et al., 2008; Raddatz et al., 2014; Rüggeberg et al., 2007), sediment supply (De Mol et al., 2007; Wheeler, Kozachenko, et al., 2005) and biological processes (Wienberg et al., 2008). Furthermore, a number of mound-development models linked to glacial-interglacial cycles have been presented (Douarin et al., 2014; Eisele et al., 2008; Roberts et al., 2009; Wheeler and Stadnitskaia, 2011).

Advances in marine survey technologies and techniques have fostered novel research opportunities to help better understand the marine environment, particularly in cold-water coral habitats (e.g. Freiwald and Wilson, 1998; Mangini et al., 1998; Mortensen et al., 2001; Roberts et al., 2009). As such, marine remotely-sensed mapping of CWC habitats is becoming progressively more common through the use of side scan sonar (SSS) and multibeam echosounders (MBES). For example, Huvenne et al. (2005) examine the influence of currents and sediment dynamics on the growth of coral and mound development at a mound province scale whereas Dorschel et al. (2009) provide an environmental context to cold-water coral carbonate mound development, both using regional SSS mapping (TOBI 30 kHz SSS). More recently, increased resolution (0.2 m x 0.2 m) SSS surveying has allowed for detailed inspections of coral habitat change in Marine Protected Area's over relatively short timescales (Huvenne et al., 2016). MBES has also proven an integral part of marine habitat mapping for CWC habitats using hull-mounted (Beyer et al., 2003), ROV-mounted (Dolan et al., 2008; Lim et al., 2017), AUV-mounted (Correa et al., 2012) and forward-facing MBES systems (Huvenne et al., 2011).

With recent advances in more accurate underwater positioning for deployed marine sampling/surveying equipment (Chitre et al., 2008; Kinsey et al., 2006), ground-truthing of

marine remotely-sensed mapping coverages is now possible with the effective positioning of still camera and video (ROV and drop frame). ROV video has proven useful in both covering large areas (Guinan et al., 2009; Huvenne et al., 2005) and providing baseline studies (Vertino et al., 2010) within CWC habitats. More recently, techniques for imaging complex structures in difficult, deep-water environments has become better developed at higher resolutions (e.g. Robert et al., 2017).

Temporal variability across CWC habitats has been studied at various scales. Lavaleye et al. (2009) utilize long time-series datasets to understand CWC habitat functioning and its effect on the organic biochemistry of the mound-influencing water column. Anthropogenic impact (trawling activities and drill cutting) at CWC habitats have driven some temporal variability research. However, these studies reveal information about temporal mound surface change utilising different approaches to video inspection at 1, 4 or 10 year timescales (Huvenne et al., 2016; Lundälv et al., 2008; Purser, 2015).

It is now more common to map (bathymetry and backscatter), physically sample (coring and grabs) and image (ROV video) CWC habitats for research purposes. Various combinations of these data types at differing resolutions in different geographic settings, and quite often with a temporal gap between sampling, are utilised to make parallels and contrasts between these habitats. Although not ideal, this is often done due to the costly and time-consuming nature of deep-water data acquisition under weather- and sea state-dependant conditions. However, a common finding of this research is the heterogeneity of these habitats (Lim et al., 2017; Vertino et al., 2010; Wienberg et al., 2009) stressing the need for local-scale studies (Davies and Guinotte, 2011; Dolan et al., 2008; Robert et al., 2016) with a robust sampling density. In light of this, our aim is to identify the minimum amount of imagery needed to accurately quantify the proportion of sediment facies on surface of an individual CWC mound and assess how to best collect this imagery in a representative manner. Furthermore, CWC mounds exist in

dynamic environments but how rapidly do these mounds change? Growth rates of corals give us a clue but how does that translate into full-mound surface change? This study therefore also assesses relative temporal change in mound surface facies and uses this data to assess the temporal consistency of data. However, this method should be corroborated in other areas to assess its robustness.

2 Materials and Methods

2.1 Study Site

The Piddington Mound, a CWC mound in the Belgica Mound Province (BMP), has been selected for this study due to the existence of high-resolution imagery (Video and bathymetry) with sufficient spatial mound coverage as presented in Lim et al. (2017). The BMP is located on the eastern slope of the Porcupine Seabight, NE Atlantic (Fig. 1). Previously designated as a Special Area of Conservation (SAC) under the EU Habitats Directive, the BMP hosts 2 chains of contour-parallel giant CWC carbonate mounds ranging in height from 50 m to 100 m and having a slight elongate to conical morphology (Wheeler, Kozachenko, et al., 2005). A salinity maximum from 600 m to 1000 m water depth marks the depth range of the Mediterranean Outflow Water (MOW), the main mound-influencing water mass in the BMP where intermediate nepheloid layers increase food availability and lateral transport of coral larvae and therefore, influencing their distribution (Dullo et al., 2008; White, 2007).

Between and around these chains of giant CWC carbonate mounds, are approximately 250 CWC mounds, referred to as the "Moira Mounds" (Wheeler et al., 2011) of which the Piddington Mound is an example. They are small (typically ~10 m tall and 40 m x 60 m in areal extent) with an ovoid to elongate morphology. It is speculated that they are Holocene in age (Huvenne et al., 2005). They exist in various different settings: at the head of sediment wave trains, within a blind channel, around barchan sediment waves or on gravel ridges and

occur as isolated or, more commonly, clustered examples (Wheeler, Beck, et al., 2005). They can be divided into 4 different areas based on their geographic distribution: the upslope area, the northern area, the downslope area and the midslope area. The Moira Mounds within the downslope area, where the Piddington Mound resides, are concentrated within part of the Arwen Channel (Murphy and Wheeler, 2017; Van Rooij, 2004). This area has been described as favourable for CWC mound development with current speeds of approximately 40 cm s^{-1} (Lim, 2017). The surrounding seabed is dominated by dropstones while the Piddington Mound itself is dominated by *Lophelia pertusa* and *Madrepora oculata* colonies. It has four distinct facies (live coral framework, dead coral framework, coral rubble and hemipelagic sediment with dropstones) occurring in a ring-like distribution around the mound summit (Lim et al., 2017).

<Insert Figure 1>

2.2 Video data

Two ROV-video datasets were collected for this research. The first video dataset (referred to from here on as "T1") was collected during the *VENTuRE survey* (2011) on board *RV Celtic Explorer* with the *Holland 1 ROV* (cruise number CE11009: Wheeler and shipboard party, 2011). The second video dataset (referred to from here on as "T4") was collected during the *QuERCi survey* (2015) on board *RV Celtic Explorer* with the *Holland 1 ROV* (cruise number CE15009: Wheeler and shipboard party, 2015). Both research cruises collected video data over the Piddington Mound using a downward-facing HD camera mounted on the bottom of the ROV. Positioning and navigation for the ROV during dives were achieved using a Sonardyne Ranger 2 USBL (ultra-short baseline positioning system) corrected by RDI Workhouse doppler velocity logger. The ROV altimeter recorded and logged the height of the ROV (and therefore camera) above the seabed. The ROV recorded downward-facing HD video during a series of

147 transects covering the entire surface of the Piddington Mound. To maintain a clear image of
148 the mound surface, the ROV was flown <2 m above the mound surface at a survey speed of <2
149 knots. Several lights were attached to the ROV to achieve homogenous lighting across the
150 camera field of view.

151 The T1 ROV-video dataset was converted into a video mosaic (Lim, 2017; Lim et al., 2017)
152 using the IFREMER in-house software *Matisse* where the images were extracted from the raw
153 video data at a rate of 1 per second. Poor quality video data (from imagery flown at over 2 m
154 above the seabed, or collected in poor water quality or with poor navigation) were excluded
155 from the image extraction process. To lower ROV trajectory noise, all the USBL navigation
156 data were filtered using a sliding median filtering and 2nd order polynomial model fit. The
157 extracted images and filtered navigation were then synced so each image had an approximate
158 position, which is later refined by the mosaicking process. At this point, features in the
159 extracted images were both detected and matched using a SIFT (Scale Invariant Feature
160 Transform) Algorithm (Lowe, 1999). Image matching and USBL navigation were merged to
161 give an accurate global position, correct scaling and sufficient local overlapping through a cost
162 function minimisation. This method is similar to Ferrer et al. (2007) except cost function
163 weights are affected according to image and navigation data standard deviations so re-
164 projection errors are minimized in the mosaicking plane rather than the image plane. After the
165 image positions are refined, the mosaic can be drawn incorporating seaming and blending
166 techniques developed by Burt and Adelson (1983) and Kwatra et al. (2003). The resulting video
167 mosaic is shown in Figure 2.

<Insert Figure 2>

168

169 The georeferenced T1 video mosaic was imported to ArcMap where a fishnet made up of 0.25
170 m^2 cells was overlaid on the Piddington Mound mosaic. A manual classification was carried
171 out on the mosaic using the following classifiers: “hemipelagic sediment with dropstones”,
172 “coral rubble”, “hemipelagic sediment”, “dead coral framework” and “live coral framework”
173 (see Fig. 2). The classified fishnet was saved as a shapefile and plotted in ArcMap (Fig. 3).

174

<Insert Figure 3 >

175 2.3 Image sampling analysis

176 To determine the minimum amount of imagery (photographic or still-video) needed from the
177 Piddington Mound to accurately characterise the diversity of surface facies present, sample size
178 estimation (specific to multinomial proportions) was carried out according to Thompson
179 (1987). While other sample size estimation techniques exist (e.g. Angers, 1974), this particular
180 technique is chosen for its robustness and accuracy even in worst case scenarios i.e. when the
181 population proportions (in this case facies proportions) are all equal. The classified cells from
182 the Piddington Mound describe a multinomial distribution with 6 different classes:
183 “hemipelagic sediment with dropstones”, “coral rubble”, “hemipelagic sediment”, “dead coral
184 framework”, “live coral framework” and “no data” (where there is a data gap as a result of data
185 quality being too low to mosaic). To do this, the confidence interval accuracy was defined by
186 selecting an alpha level (α), which represents the significance level at which the confidence
187 level is calculated (e.g. an alpha level of 0.05 gives a confidence level of 95%) and margin of
188 error (d). This ensured the probability that population proportions (facies proportions) across
189 the whole mound surface were covered by the confidence interval. Thompson (1987) provides
190 a table showing the minimum sample size required once these values are defined (see Table 1).
191 For this study, a confidence interval of 95% was defined (i.e. α of 0.05) with a margin of error

192 (d) of 0.05 allowing a sample size, *X* (n if d=0.05), to be determined (see Table 1). Note, both
193 smaller values of α and smaller margins of error (d) would require larger sample sizes (*X*) and
194 this method does not take into account spatial autocorrelation. This does not appear to be an
195 issue as all results occur within the 95% confidence interval regardless.

<Insert Table 1>

196 To determine the best method for collecting images of the mound surface to most effectively
197 capture mound heterogeneity, a series of potential survey designs were performed for the
198 Piddington Mound in ArcMap and saved as *.shp files (Fig. 4). These are used as a guide for
199 a hypothetical drop camera system or ROV to acquire downward-facing stills or live video
200 from which stills can be extracted. The survey designs include the following: a) SD1 - random
201 points; b) SD2 - south to north transect; c) SD3 - east to west transect; d) SD4 - northwest-
202 southeast diagonal transect; e) SD5 - 2 lines; f) SD6 - 3 straight, parallel line grid; g) SD7 - 3
203 summit-crossing lines; h) SD8 - horizontal grid; i) SD6 - spiral (circling from the mound base
204 to the mound summit) and; j) SD7 - actual survey example (taken from ROV reconnaissance
205 dive navigation over the Piddington Mound). Using the "create random points" tool in ArcMap,
206 *X* number of random points were generated across the surface of the Piddington Mound (SD1).
207 To collect random points from anywhere on the mound surface, the full mound surface must
208 therefore be imaged thus, SD1 represents the scenario of having full-mound video mosaic
209 coverage. Then, to represent each of the other scenarios, *X* number of random points were
210 generated across the fishnet but restricted to the lines defining each survey design *.shp file
211 (SD2 to SD10: Figure 4). The proportion of cells of each class for each survey design was
212 calculated. The total number of 0.25 m^2 cells in the fishnet from each class were also counted
213 and the proportion of these cells calculated. This acts as the real-life control against which

results from each survey design can be compared. The results were graphed and the number of "no data" values recorded within each survey design are used to generate proportional error bars for each individual class.

<Insert Figure 4>

2.4 Temporal variability analysis

A repeat survey of the Piddington Mound was undertaken four years after T1 and termed T4. The T4 survey comprises parallel north-south video lines covering the whole mound. In line with the image sampling analysis methodology established herein, a minimum of number of images (X) were extracted from the T4 ROV video dataset with an equal number of images extracted from each video line to ensure a homogenous spread of images across the Piddington Mound surface. The video lines covering 100% of the mound, offer a comparison of the T1 Piddington Mound mosaic after a 4-year interval and in survey design is comparable to "SD1 - random points".

Each extracted image was manually inspected. A cell (25 cm x 25 cm) is overlaid around the area of the photo where the laser scales pointed (central field of view) and a manual classification was applied using the same classifiers as the T1 ROV video data set: "hemipelagic sediment with dropstones", "coral rubble", "hemipelagic sediment", "dead coral framework" and "live coral framework". The total number of cells from each class were counted and their proportion determined.

3 Results

3.1 Seabed classification

Figure 3 shows the classified fishnet over the Piddington Mound. 6 classes exist: “hemipelagic sediment with dropstones”, “coral rubble”, “hemipelagic sediment”, “dead coral framework”, “live coral framework” and “no data”. These classes are described in Table 2. There are 5637 cells across the surface of Piddington Mound with the most common being “coral rubble” (36.1 ± 3.13%) and “dead coral framework” (31.6 ± 2.74%). The least common cell-types are “hemipelagic sediment” (1.1 ± 0.09%) and “hemipelagic sediment with dropstones” (6.7 ± 0.58%). The “live coral framework” cells cover 16.3 ± 1.42% of the mound surface. While the “coral rubble” cell-type is found across the mound surface, it is typically concentrated around the mound perimeter and on the mound summit. The “live coral framework” cells occur most frequently towards the north of the mound. The “dead coral framework” can be found on the mound flanks. For the remainder of the text, the proportions of all observed cell-types on the Piddington Mound are referred to as the *control proportion*.

<Insert Table 2>

3.2 Image sampling analysis

Sample size estimation according to Thompson (1987), reveals a sample size, *X* (n if d=0.05), of 510 as a minimum sample size to reliably replicate, with a confidence level of 95%, the proportion of facies in the total of 5637 classified cells in the 0.25 m^2 fishnet overlay on the T1 Piddington Mound video-mosaic. The number of categories in our sample size is 6 which is greater than the required minimum of 3.

255 Figure 5 shows the results of the image sampling analysis for each survey design (more
256 information can be found in the supplementary data supplied with the online version) as facies
257 sampling curves. Survey design "SD1 - random points" (Fig. 5A) represents maximum video
258 coverage and thus the ability to drop 510 random points anywhere across the Piddington
259 Mound surface. This survey design resulted in a 5.9% total difference in facies from the control,
260 namely of the actual proportion of all cells covering the Piddington Mound. The maximum
261 difference in an individual class is 2.9% ("dead coral framework") with an average class
262 difference of 1.2%.

<Insert Figure 5 >

263 Survey design "SD2 - south to north transect" (Fig. 5B) represents 510 random image sampling
264 points anywhere along a straight, individual ROV video line from the southern end to the
265 northern end of the Piddington Mound. The line is 50 m in length taking approx. 3.2 minutes
266 for an ROV to complete at 0.5 knots. This survey design resulted in a total of 22.5% difference
267 to that of the actual proportion of all cells covering the Piddington Mound. The maximum
268 difference in an individual class is 6.3% ("dead coral framework") with an average class
269 difference of 4.1%.

270 Survey design "SD3 - east to west transect" (Fig. 5C) represents 510 random image sampling
271 points anywhere along a straight, individual ROV video line from the eastern edge to the
272 western edge of the Piddington Mound. The line is 40 m in length taking approx. 2.5 minutes
273 for an ROV to complete at 0.5 knots. This survey design resulted in a total of 11.8% difference
274 to that of the actual proportion of all cells covering the Piddington Mound. The maximum
275 difference in an individual class is 5.8% ("hemipelagic sediment with dropstones") with an
276 average class difference of 1.7%.

Survey design “SD4 - northwest-southeast diagonal transect” (Fig. 5D) represents 510 random image sampling points anywhere along a straight, individual ROV video line from the north-western edge to the south-eastern edge of the Piddington Mound. The line is 40 m in length taking approx. 2.5 minutes for an ROV to complete at 0.5 knots. This survey design resulted in a total of 22.4% difference to that of the actual proportion of all cells covering the Piddington Mound. The maximum difference in an individual class is 7.6% (“live coral framework”) with an average class difference of 2.9%.

Survey design “SD5 - 2 lines” (Fig. 5E) represents 510 random image sampling points anywhere along 2 straight ROV video lines (SD2 + SD3) intersecting each other at the summit of the Piddington Mound. This survey covers a line length of 90 m taking approx. 5.8 minutes for an ROV to complete at 0.5 knots. This survey design resulted in a total of 12.4% difference to that of the actual proportion of all cells covering the Piddington Mound. The maximum difference in an individual class is 4.7% (“hemipelagic sediment with dropstones”) with an average class difference of 2.0%.

Survey design “SD6 - 3 straight, parallel line grid” (Fig. 5F) represents 510 random image sampling points anywhere along 3 straight, parallel ROV video lines traversing the Piddington Mound in a north-south orientation. This survey covers a line length of 130 m taking approx. 8.4 minutes for an ROV to complete at 0.5 knots. This survey design resulted in a total of 22.9% difference to that of the actual proportion of all cells covering the Piddington Mound. The maximum difference in an individual class is 9.7% (“hemipelagic sediment with dropstones”) with an average class difference of 3.8%.

Survey design “SD7 - 3 summit-crossing lines” (Fig. 5G) represents 510 random image sampling points anywhere along 3 straight, parallel ROV video lines traversing the Piddington Mound (SD2 + SD3 + SD4). This survey covers a line length of 130 m taking approx. 8.4

minutes for an ROV to complete at 0.5 knots. This survey design resulted in a total of 11.1% difference to that of the actual proportion of all cells covering the Piddington Mound. The maximum difference in an individual class is 3.4% ("dead coral framework") with an average class difference of 1.8%.

Survey design "SD8 - horizontal grid" (Fig. 5H) represents 510 random image sampling points anywhere along an east-west grid of ROV video lines covering the Piddington Mound. This survey covers a line length of 320 m taking approx. 20.7 minutes for an ROV to complete at 0.5 knots. This survey design resulted in a total of 5.8% difference to that of the actual proportion of all cells covering the Piddington Mound. The maximum difference in an individual class is 2.9% ("coral rubble") with an average class difference of 1.1%. It is also worth noting that there was 0% cell difference in 3 classes.

Survey design "SD9 - spiral" (Fig. 5I) represents 510 random image sampling points anywhere along a spiral or conical ROV video line circling from the mound perimeter to the mound flank to the mound summit. This survey covers a line length of 240 m taking approx. 15.5 minutes for an ROV to complete at 0.5 knots. This survey design resulted in a total of 13.4% difference to that of the actual proportion of all cells covering the Piddington Mound. The maximum difference in an individual class is 4.1% ("dead coral framework") with an average class difference of 2.2%.

Survey design "SD10 - actual survey example" (Fig. 5J) represents 510 random image sampling points along an actual ROV reconnaissance dive video line over the Piddington Mound. This survey covers a line length of 1283 m taking 83 minutes for the ROV to complete at 0.5 knots. This survey design resulted in a total of 17.7% difference to that of the actual proportion of all cells covering the Piddington Mound. The maximum difference in an

individual class is 6.7% ("hemipelagic sediment with dropstones") with an average class difference of 3.4%.

3.3 Temporal variability analysis

Figure 6 and Table 3 show the results of the temporal variability of the Piddington Mound surface data based on a comparison to class determinations in the T1 and T4 video survey data. The minimum number of random samples needed to characterise the mound with a 0.95 probability of being within 0.05 of the class proportions is 510. Here, 622 images are used which marginally increases accuracy above 95% confidence. The most common T4 cell-types are "coral rubble" (43.6%) and "dead coral framework" (37.3%). The "live coral framework" cell-type occurs 16.7% of the time. The least common cell types are "hemipelagic sediment" (1%) and "hemipelagic sediment with dropstones" (1.4%). An important limiting factor of this result is that the error bars developed (Fig. 6 and Table 3) must be considered when comparing the T1 and T4.

<Insert Figure 6>

<Insert Table 3>

4 Discussion

4.1 Seabed imagery for cold water coral mound characterisation

Numerous CWC mounds have been studied incorporating video observations from ROV-mounted camera systems in various different ways: oblique-angled, forward-facing camera

(Foubert et al., 2005), downward-facing camera (Huvenne et al., 2016), both downward-facing and oblique-angled, forward-facing cameras (Dolan et al., 2008; Guinan et al., 2009) and up to 3 cameras (Savini et al., 2014; Vertino et al., 2010). In this study, we focus only on downward facing cameras and we question the effect of the amount of imagery used and the survey design by which it was collected which often varies from study to study. Here, the amount and survey design of seabed imagery acquisition is examined to put forward a survey-feasible methodology for characterising the surface of CWC mounds.

4.1.1 How much seabed imagery is needed to characterise the Piddington Mound?

In the deep sea, sampling and surveying opportunities are limited due to the availability, financial expense and weather-dependency of ship-time on research vessels. As a result, deep-marine data collection is strictly prioritised by urgency of data needs, quite often to meet the needs of funding sources. As such, studies have used "single-pass" (individual line, typically straight) video lines across the surface of CWC mounds to ground truth their surface (e.g. Foubert et al., 2005; Huvenne et al., 2016). While this offers the opportunity to increase the geographical range of the study, it decreases the potential confidence and representativeness of the study. This leads to the question, how much imagery is actually needed to create a reliable representation of the surface of a CWC mound?

Based on the seabed classification (Figure 3), the mound surface sediment facies proportion of 0.25 cm^2 cell-types on the Piddington Mound are known. Our sample size estimation shows that 510 is the minimum number of 0.25 cm^2 images needed to accurately determine the proportion of identified classes on the Piddington Mound. Survey design "SD1 - random points" represents the ability to drop 510 random points anywhere on the Piddington Mound, thus utilizing the same video coverage as the T1 ROV video data set (full mound coverage).

Therefore, it can be used to assess and ground-truth the accuracy of the determined sample size. A comparison of the control proportion (Figure 5; All T1) with survey design "SD1 - random points" (Figure 5) shows that this estimation is within 5.9% of the correct proportion of cell-types observed on the Piddington Mound, in line with the aimed probability (at least 0.95 that all estimates are within 0.05 of the multinomial proportions) of this dataset and gives the most reliable representation of the mound surface of all the survey designs tested. The "SD1 - random points" survey could be accomplished by sub-sampling a video-mosaic (100% mound coverage) which, perhaps not surprisingly, is the most robust approach to characterising the mound surface. This could alternatively be accomplished by the use a yo-yo drop camera.

Vertino et al. (2010) examine CWC meso- and macro-scale habitats at the Santa Maria di Leuca Coral Province, a clear example of the utilisation of dense ROV video coverage on CWC mounds and associated habitats to produce detailed studies. The detail revealed by studies with dense video coverage per CWC mound raises the question: are the spatial representation of "single-pass" video line surveys across CWC mounds enough? And conversely, with strict research cruise schedules, at what point does video coverage become *excessive*?

Single-pass ROV video lines across CWC mounds are common (i.e. Dolan et al., 2008; Lim, 2017). As such, 3 different straight line survey designs are tested here ("SD2 - south to north", "SD3 - east to west" and "SD4 - northwest-southeast diagonal transect") (Fig. 4 and 5). With an average of 18.9% total difference in cell-type proportions from the control proportion, single-pass surveys appear to yield the least representative results. This is expected given the reduced spatial representation of such survey designs. Two of these survey designs ("SD2 - south to north" and "SD4 - northwest-southeast diagonal transect") produce a total difference of 22.5% and 22.4% in cell-type proportion from the control proportion, while "SD3 - east to west" produces a total difference of 11.8%. The ring-like cell-type clustering that exists on the Piddington Mound (Lim et al., 2017) appears to have an influence on this result as the course

of the east to west line happens to cover an area with similar proportions to the control proportion. This is evidenced by approximately 50% of the total difference of this survey design resulting from 1 individual facies.

"SD5 - 2 lines" demonstrates the effect of adding a second line to one of these single-pass ROV video lines, in this case SD2 and SD3. This shows an increase in accuracy of 6.5% from single pass surveys (18.9%) to the 2 line survey (12.4%). "SD7 - 3 summit crossing lines" demonstrates the effect of adding a third line (SD2 + SD3 + SD4) to these 2 lines. This shows an increase in accuracy of 1.3% from the 2 line (12.4%) (SD 2 + SD3) survey to the 3 line (11.1%) (SD2 + SD3 + SD4) survey. As such, doubling the number of lines from 1 to 2 increased the accuracy by 6.5% while adding the third line increased the accuracy by just 1.3% while adding 2.6 minutes of extra survey time. Interestingly, a comparison of these 3 summit-crossing lines with 3 lines collected in a grid (SD6), both surveys the same length and time (130 m; 8.4 minutes), highlights the effect of survey design on results where "SD6 - 3 line grid" produced notably less-accurate results (22.9% total difference in facies proportions from the control proportion).

Another common survey design is following the geomorphology of the CWC mound (i.e. Guinan et al., 2009) or some other known characteristic. In the case of the Piddington Mound, survey design "SD9 - spiral" (Fig. 4 and 5) follows both the bathymetry and ring-like growth already observed on the Piddington Mound (Lim et al., 2017), circling through the mound perimeter, flank and summit. This cone-like survey design yields a 13.4% total cell-type proportion difference from the control proportion. The accuracy of this result is probably due to the influence of prior knowledge on survey design.

Survey design "SD10 - actual survey" defines the navigation path of an ROV on a reconnaissance dive over the Piddington Mound when it was first discovered and initially

417 investigated (Wheeler and shipboard party, 2011) (Fig. 4 and 5). This survey design yields a
418 17.7% total cell-type proportion difference from the control proportion. It represents a real-life
419 example of survey design without the influence of prior knowledge or mapping of the CWC
420 mound. This survey design (or lack of) resulted in relatively a large (7.6%) over-estimation of
421 "live coral framework" cell-types. This sampling bias may be typical of reconnaissance video
422 investigations when discovering new seabed features as scientists may preferentially
423 concentrate the cameras on the live proportion of the feature that is of more interest to them.
424 Another short-coming of this survey design, and probably a result of the same sampling bias,
425 is that 2 entire classes were not seen in the video observation ("hemipelagic sediment with
426 dropstones" and "hemipelagic sediment"). Interestingly, this survey covered a line length of
427 1283 m (83 survey minutes), over 1000 m more than the aforementioned surveys designs. As
428 such, this once again highlights the importance of survey design over line length.

429 Probably the most well-known survey design, but apparently least-applied in the case of CWC
430 mounds is survey design "SD8 - horizontal grid" (Fig. 4 and 5). In this example, the grid is
431 made up of a series of mound-traversing lines spaced approximately 5 m apart where the end
432 of each line is connected to the start of the next line. This survey design yields a 5.8% total
433 cell-type proportion difference from the control proportion, the most representative proportion
434 of the study. An additional positive of this survey design is that it estimated the exact proportion
435 of individual cell-types for 3 classes ("hemipelagic sediment with dropstones", "hemipelagic
436 sediment" and "live coral framework"). Interestingly, it also yields a similar result to survey
437 design "SD1 - random points" (5.9%) which represents full-mound video coverage. With line
438 spacing of approx. 1 m, it took ~8 hours to collect the full-mound video coverage (Wheeler and
439 shipboard party, 2011). Assuming a survey speed of 0.5 knots to collect survey design "SD8 -
440 horizontal grid" (line length of 320 m), it would take 20.7 minutes to collect this ROV video
441 data, a vast improvement from ~8 hours for the same representation of surface facies

442 proportions. In addition, this technique appears to be unbiased by the significant clustering
443 found on the Piddington Mound (Lim et al., 2017).

444

445 4.2 What is the temporal variability of Piddington Mound and its implication for samples?
446 The T4 ROV-video dataset was collected over the Piddington Mound 4 years after the T1
447 survey (2015) covering the entire mound surface with the same downward-facing camera array.
448 To assess mound surface change over this period, 622 random images are classified (a
449 minimum of 510 are needed) according to the image sampling technique established above
450 using the same classifiers. The survey design, similar to the T1 ROV video data set, covers the
451 entire mound surface by a 1 m spaced line grid. Thus, the accuracy of this data is similar to that
452 of survey design "SD1 - random points" (Fig. 5).

453 The T4 ROV video dataset exhibits a change of 19% of the total mound surface in comparison
454 to the T1 ROV video dataset. This change has taken place over 4 years (2011 - 2015) and is
455 evident at a 25 cm^2 resolution. The "live coral framework" cell-type remains relatively
456 constant, increasing by only 0.4% over the 4 years (+0.1% per year). A minute increase is
457 expected given the slow growth rates (15 - 30 mm yr^{-1}) observed in *Lophelia* (Gass and Roberts,
458 2006; Larcom et al., 2014; Orejas et al., 2008). Similarly, Huvenne et al. (2016) show that after
459 ten years, the amount of live coral found on the Darwin Mounds, the only other known example
460 of small-sized CWC mounds in the NE Atlantic, also remains the same. The "normal"
461 proportion of live coral per Darwin Mound is ~45-55%, sizably greater than that found here on
462 the Piddington Mound.

463 The "hemipelagic sediment" cell-type also remains relatively constant (-0.2% over 4 years)
464 given the minute change and size of the potential error margin (Table 3). This facies is typically
465 found in the lee of "live coral framework" cell-types (Fig. 3) where it is protected from

resuspension by the current (Lim et al., 2017). As such, given the fact that the proportion of "live coral framework" cells have not changed, it seems likely that the proportion of "hemipelagic sediment" cell-type would remain the same.

The "coral rubble" cell-type increased the most (7.5%) at a rate of 1.9% per year, assuming a constant rate of change. Given the dominance of the "coral rubble" cell-type on Piddington Mound in 2011, it is likely to see a change in the proportion of this class. The source of this coral rubble is likely to be as a result of the biological or physical erosion of the "dead coral framework" class (Lim et al., 2017) or on-mound (re)exposure and redistribution through benthic erosion and transport processes.

Interestingly, the proportion of "dead coral framework" cell-type increased by 5.7% (a rate of 1.4% per year). If this class is both contributing to the "coral rubble" class and increasing relative to the T1 "dead coral framework" class, then it can be assumed that it changed by at least 5.7% and at a minimum of 1.4% per year. Given the low growth rate of *Lophelia* mentioned earlier, it is unlikely that the source of the increased "dead coral framework" coverage is entirely from the degradation of the "live coral framework" cell-type. It is therefore suggested that this increase is possibly through "dead coral framework" exhumation by currents removing covering sediment. Although there has been impact of demersal trawling on the seabed in the area (Foubert et al., 2005; Wheeler, Beck, et al., 2005), the Belgica Mound Province is now an SAC (special area of conservation). As such, it less likely that trawling has impacted the movement of dead coral framework on the mound during the course of the study.

The proportion of the "sediment and dropstone" class decreases the most (-5.3%) at a rate of 1.3% per year. Given the mound-perimeter occurrence of this class and the dominance of the "coral rubble" on the steepest parts of the mound (flanks), it is likely that this decrease is due to burial by coral rubble where the coral rubble (or freshly eroded coral rubble from dead coral

490 frameworks) roll from the steepened mound flanks to the edges of the mound where the slope
491 decreases and “sediment and dropstone” cell-types are common (Lim et al., 2017).

492 Based on the results herein and cautiously assuming a linear rate of change of a total mound
493 surface change of 4.8% per year, then in just over 20 years, this suggests the entire Piddington
494 Mound surface will change. Thus, if physical and image (video or photographic) samples are
495 taken 5 years apart on Piddington Mound, a change of 25% (and 50% after 10 years) on the
496 mound surface influences whether or not these samples consistently represent the mounds’
497 status in the contemporary environment. This, coupled with the heterogeneity observed on the
498 CWC mounds, positioning error margins (e.g. ~2 m with some calibrated USBL systems in
499 deep water) and inconsistencies of repeat video acquisition (Purser, 2015) contests the validity
500 of interpretation from surface samples on similar CWC mounds. It is therefore recommended
501 that data from various survey campaigns should be treated cautiously as they may not represent
502 the “contemporary” environment. As such, we strongly recommend to use samples collected
503 during the same survey to represent the contemporary environment (e.g. samples collected in
504 2017 to be used only with video coverage from 2017) if possible.

505 Centimetre-scale, remotely-sensed mapping is becoming more common in the marine
506 environment. As such, observations from video data should be equally as accurate. Oblique
507 camera data acquisition induces positional errors where there is an offset between the field of
508 view of the camera and the positioning beacon (e.g. USBL) thus giving an incorrect position
509 for oblique camera video observation. This error is a function of camera obliqueness, rotation
510 of the camera-mounted platform (e.g. ROV) around its axis, seabed slope and height of camera
511 from seabed and is therefore not constant nor easily reconciled. For relevant example, oblique
512 camera data has been utilized in a temporal study of a CWC mound, offshore Norway, which
513 highlights the inconsistencies of repeat surveys using oblique camera (e.g. viewing the same
514 part of the mound from different angles) (Purser, 2015). As such, we would like to recommend

515 the use of downward-facing camera for temporal-based studies of CWC habitats (and other
516 dynamic marine habitats) as positioning of the camera is not influenced by rotation of the
517 camera around its axis, the angle at which it views the seabed is always the same (0°) and is
518 not influenced by seabed slope in the same way as oblique camera.

519 **5 Conclusion**

520 This study presents an assessment of video survey design specific to a CWC mound (the
521 Piddington Mound of the Moira Mounds, NE Atlantic) to assess both differences in surface
522 facies proportion and temporal facies proportion. The technique presented is developed with
523 particular consideration for the financial, temporal and sea-state dependant nature of deep sea
524 research to maximise resolution and spatial coverage. Known proportions of CWC-typical
525 facies on the Piddington Mound were used to determine the minimum number of images
526 needed to characterise the surface of similar-sized CWC mounds with the same number of
527 classes using downward-facing camera. This allows for a standardised approach to surveying
528 and studying CWC mounds through video and comparison of mounds in different geographic
529 settings and in time at 25 cm^2 resolution. A comparison of different common survey designs
530 show that single-pass video are the least-representative and highly-influenced by the
531 heterogeneity, typical of CWC mounds, despite being commonly utilised in research.
532 Following bathymetry or known features on CWC mounds is another common survey design
533 but does not yield the most accurate results. The most representative results were yielded from
534 either fully video mosaicking a mound or using a grid of spaced lines. However, a grid of lines
535 in this case requires 1/16 of the time required for video mosaicking an entire mound while
536 yielding similar results.

537 The developed technique was applied to the Piddington Mound 4 years later to assess the
538 change in proportions of facies across the mound surface. With a mound surface change of

4.8% per year, the mound surface has changed by almost 20% from 2011 to 2015. The greatest change was in the "coral rubble" class (7.5%) followed by "dead coral framework" and "sediment and dropstone" classes. These classes are affected by strong currents as mobile or exhumed substrates. Similar to other mounds, the proportion of "live coral framework" class remained the same over the 4-year period as anticipated for a sessile slow growing organism. Although assuming a linear rate of change, we suggest that in approx. 20 years, ~100% change in the surface of the Piddington Mound. Thus, samples taken from the mound 5 years apart (with a 25% mound surface change), makes the samples inconsistent and therefore not representative of the contemporary mound status. We also stress that in utilising this technique, the potential error bars must be taken into consideration when comparing between data sets. Finally, we highlight the suitability of downward-facing camera for high-resolution repeat surveys for temporal variability purposed due to the many short-comings of temporal-based, oblique-camera surveys.

6 Acknowledgements

The authors would like to sincerely thank Boris Dorschel for his extremely useful input and proofing of this work, Evan Edinger and another anonymous reviewer for their timely and insightful reviews. We would like to thank the crew and officers of ROV Holland 1 and RV Celtic Explorer for assistance in collecting high resolution, accurately positioned data. Ship time on the RV Celtic Explorer was funded by the Marine Institute under the 2011 and 2015 Ship Time Programme of the National Development Plan. Mohit Tunwal (UCC) is thanked for mathematical proofing.

7 References

Angers, C., 1974. A graphical method to evaluate sample sizes for the multinomial distribution. Technometrics 16, 469-471, http://dx.doi.org/10.1080/00401706.1974.10489219.

Beyer, A., Schenke, H.W., Klenke, M., Niederjasper, F., 2003. High resolution bathymetry of the eastern slope of the Porcupine Seabight. Marine Geology 198, 27-54, http://dx.doi.org/10.1016/S0025-3227(03)00093-8.

Burt, P.J., Adelson, E.H., 1983. A Multiresolution Spline with Application to Image Mosaics. Acm Transactions on Graphics 2, 217-236, Doi 10.1145/245.247.

Chitre, M., Shahabudeen, S., Stojanovic, M., 2008. Underwater acoustic communications and networking: Recent advances and future challenges. Marine Technology Society Journal 42, 103-116, http://dx.doi.org/10.4031/002533208786861263.

Correa, T.B.S., Eberli, G.P., Grasmueck, M., Reed, J.K., Correa, A.M.S., 2012. Genesis and morphology of cold-water coral ridges in a unidirectional current regime. Marine Geology 326, 14-27, 10.1016/j.margeo.2012.06.008.

Davies, A.J., Guinotte, J.M., 2011. Global Habitat Suitability for Framework-Forming Cold-Water Corals. PLoS ONE 6, e18483, 10.1371/journal.pone.0018483.

Davies, A.J., Wisshak, M., Orr, J.C., Roberts, J.M., 2008. Predicting suitable habitat for the cold-water coral *Lophelia pertusa* (Scleractinia). Deep-Sea Research I 55, 1048-1062, http://dx.doi.org/10.1016/j.dsr.2008.04.010.

De Mol, B., Kozachenko, M., Wheeler, A.J., Alvares, H., Henriet, J.-P., Olu-Le Roy, K., 2007. Thérèse Mound: a case study of coral bank development in the Belgica Mound Province, Porcupine Seabight. International Journal of Earth Sciences 96, 103-120, http://dx.doi.org/10.1007/s00531-005-0496-x.

Dolan, M.F.J., Grehan, A.J., Guinan, J.C., Brown, C., 2008. Modelling the local distribution of cold-water corals in relation to bathymetric variables: Adding spatial context to deep-sea video data. Deep-Sea Research I 55, 1564-1579, http://dx.doi.org/10.1016/j.dsr.2008.06.010.

Dorschel, B., 2003. Late Quaternary Development of a deep-water Carbonate Mound in the northeast Atlantic, RCOM-Bremen. University of Bremen, bremen, p. 90.

Dorschel, B., Wheeler, A.J., Huvenne, V.A.I., de Haas, H., 2009. Cold-water coral mounds in an erosive environmental setting: TOBI side-scan sonar data and ROV video footage from the northwest Porcupine Bank, NE Atlantic. Marine Geology 264, 218-229, 10.1016/j.margeo.2009.06.005.

Douarin, M., Sinclair, D.J., Elliot, M., Henry, L.-A., Long, D., Mitchison, F., Roberts, J.M., 2014. Changes in fossil assemblage in sediment cores from Mingulay Reef Complex (NE Atlantic): Implications for coral reef build-up. Deep Sea Research Part II: Topical Studies in Oceanography 99, 286-296, http://dx.doi.org/10.1016/j.dsr2.2013.07.022.

Dullo, W.-C., Flögel, S., Rüggeberg, A., 2008. Cold-water coral growth in relation to the hydrography of the Celtic and Nordic European continental margin. Marine Ecology Progress Series 371, 165-176, 10.3354/meps07623.

Eisele, M., Hebbeln, D., Wienberg, C., 2008. Growth history of a cold-water coral covered carbonate mound - Galway Mound, Porcupine Seabight, NE-Atlantic. Marine Geology 253, 160-169, 10.1016/j.margeo.2008.05.006.

Ferrer, J., Elibol, A., Delaunoy, O., Gracias, N., Garcia, R., 2007. Large-area photo-mosaics using global alignment and navigation data, MTS/IEEE OCEANS Conference, Vancouver, Canada, pp. 1-9, http://dx.doi.org/10.1109/OCEANS.2007.4449367.

Foubert, A.T.G., Beck, T., Wheeler, A.J., Opderbecke, J., Grehan, A., Klages, M., Thiede, J., Henriet, J.-P., Polarstern ARK-XIX/3a shipboard party, 2005. New view of the Belgica Mounds, Porcupine Seabight, NE Atlantic: preliminary results from the Polarstern ARK-XIX/3a ROV cruise, in: Freiwald, A., Roberts, J.M. (Eds.), Deep-water corals and Ecosystems, . Springer-Verlag, Berlin Heidelberg, pp. 403-415.

Freiwald, A., 2002. Reef-Forming Cold-Water Corals, in: Wefer, G., Billett, D.S.M., Hebbeln, D., Jørgensen, B.B., van Weering, T.C.E. (Eds.), Ocean Margin Systems, Hanse Conference on Ocean Margin Systems (2000: Delmenhorst, Germany) ed. Springer, Berlin Heidelberg New York, pp. 365-385, http://dx.doi.org/10.1007/978-3-662-05127-6_23.

Freiwald, A., Fosså, J.H., Grehan, A., Koslow, T., Roberts, J.M., 2004. Cold-water Coral Reefs, NEP-WCMC, Cambridge, UK, p. 88, http://hdl.handle.net/20.500.11822/8727.

Freiwald, A., Wilson, J.B., 1998. Taphonomy of modern, deep, cold-temperate water coral reefs. Historical Biology 13, 37-52, http://dx.doi.org/10.1080/08912969809386571.

Gass, S.E., Roberts, J.M., 2006. The occurrence of the cold-water coral Lophelia pertusa (Scleractinia) on oil and gas platforms in the North Sea: Colony growth, recruitment and environmental controls on distribution. Marine Pollution Bulletin 52, 549-559, http://dx.doi.org/10.1016/j.marpolbul.2005.10.002.

Guinan, J., Grehan, A.J., Dolan, M.F.J., Brown, C., 2009. Quantifying relationships between video observations of cold-water coral cover and seafloor features in Rockall Trough, west of Ireland. Marine Ecology Progress Series 375, 125-138, 10.3354/meps07739.

Henriet, J.P., Hamoumi, N., Da Silva, A.C., Foubert, A., Lauridsen, B.W., Rüggeberg, A., Van Rooij, D., 2014. Carbonate mounds: From paradox to World Heritage. Marine Geology 352, 89-110, http://dx.doi.org/10.1016/j.margeo.2014.01.008.

Huvenne, V.A., Tyler, P.A., Masson, D.G., Fisher, E.H., Hauton, C., Huhnerbach, V., Le Bas, T.P., Wolff, G.A., 2011. A picture on the wall: innovative mapping reveals cold-water coral refuge in submarine canyon. PLoS ONE 6, e28755, 10.1371/journal.pone.0028755.

Huvenne, V.A.I., Bett, B.J., Masson, D.G., Le Bas, T.P., Wheeler, A.J., 2016. Effectiveness of a deep-sea cold-water coral Marine Protected Area, following eight years of fisheries closure. Biological Conservation 200, 60-69, 10.1016/j.biocon.2016.05.030.

Huvenne, V.A.I., Beyer, A., de Haas, H., Dekindt, K., Henriet, J.-P., Kozachenko, M., Olu-Le Roy, K., Wheeler, A.J., participants, T.P.c., participants, C.c., 2005. The seabed appearance of

637 different coral bank provinces in the Porcupine Seabight, NE Atlantic: results from sidescan
638 sonar and ROV seabed mapping, in: Freiwald, A., Roberts, J.M. (Eds.), Cold-water Corals and
639 Ecosystems. Springer-Verlag, Berlin Heidelberg, pp. 535-569, http://dx.doi.org/10.1007/3-
640 540-27673-4_27.

641 Kinsey, J.C., Eustice, R.M., Whitcomb, L.L., 2006. A survey of underwater vehicle navigation:
642 Recent advances and new challenges, IFAC Conference of Manoeuvering and Control of
643 Marine Craft.

644 Kwatra, V., Schödl, A., Essa, I., Turk, G., Bobick, A., 2003. Graphcut textures: image and
645 video synthesis using graph cuts, ACM Transactions on Graphics (TOG). ACM, pp. 277-286,
646 http://dx.doi.org/10.1145/882262.882264.

647 Larcom, E.A., McKean, D.L., Brooks, J.M., Fisher, C.R., 2014. Growth rates, densities, and
648 distribution of Lophelia pertusa on artificial structures in the Gulf of Mexico. Deep-Sea
649 Research Part I-Oceanographic Research Papers 85, 101-109, 10.1016/j.dsr.2013.12.005.

650 Lavaleye, M., Duineveld, G., Lundälv, T., White, M., Guihen, D., Kiriakoulakis, K., Wolff,
651 G.A., 2009. Cold-Water Corals on the Tisler Reef-preliminary observations on the dynamic
652 reef environment. Oceanography 22, 76-84, http://dx.doi.org/10.5670/oceanog.2009.08.

653 Lim, A., 2017. Spatio-temporal patterns and controls on cold-water coral reef development:
654 the Moira Mounds, Porcupine Seabight, NE Atlantic, School of Biological, Earth and
655 Environmental Sciences. University College Cork, Cork Open Research Archive, p. 221,
656 http://hdl.handle.net/10468/4031.

657 Lim, A., Wheeler, A.J., Arnaubec, A., 2017. High-resolution facies zonation within a cold-
658 water coral mound: The case of the Piddington Mound, Porcupine Seabight, NE Atlantic.
659 Marine Geology 390, 120-130, https://doi.org/10.1016/j.margeo.2017.06.009.

660 Lowe, D.G., 1999. Object recognition from local scale-invariant features, Computer vision,
661 1999. The proceedings of the seventh IEEE international conference on Computer Vision. Ieee,
662 pp. 1150-1157, http://dx.doi.org/10.1109/ICCV.1999.790410.

663 Lundälv, T., Fosså, J.H., Buhl Mortensen, P., Jonsson, L.G., White, M., Guihen, D., Unnithan,
664 V., 2008. Development in a trawl-damaged coral habitat (Tisler reef, NE Skagerrak) during
665 four years of trawl protection, 4th International Symposium on Deep-Sea Corals, Wellington,
666 New Zealand, December 2008.

667 Mangini, A., Lomitschka, M., Eichstädter, R., Frank, N., Vogler, S., Bonani, G.G., Hajdas, I.,
668 Pätzold, J., 1998. Coral provides age of deep water. Nature 392,
669 http://dx.doi.org/10.1038/32804.

670 Mortensen, P.B., Hovland, M.T., Fosså, J.H., Furevik, D.M., 2001. Distribution, abundance
671 and size of *Lophelia pertusa* coral reefs in mid-Norway in relation to seabed characteristics.
672 Journal of the Marine Biological Association of the UK Volume 81, Issue 04, Aug 2001, 581-
673 597, http://dx.doi.org/10.1017/S002531540100426X.

674 Murphy, P., Wheeler, A.J., 2017. A GIS-based application of drainage basin analysis and
675 geomorphometry in the submarine environment: The Gollum Canyon System, North-east
676 Atlantic, in: Bartlett, D., Celliers, L. (Eds.), Geoinformatics for Marine and Coastal

677 Management. CRC Press, Taylor & Francis Group, Boca Raton, USA,
678 http://dx.doi.org/10.1201/9781315181523-4.

679 Orejas, C., Gori, A., Gili, J.M., 2008. Growth rates of live Lophelia pertusa and Madrepora
680 oculata from the Mediterranean Sea maintained in aquaria. Coral Reefs 27, 255-255,
681 10.1007/s00338-007-0350-7.

682 Orejas, C., Gori, A., Rad-Menendez, C., Last, K.S., Davies, A.J., Beveridge, C.M., Sadd, D.,
683 Kiriakoulakis, K., Witte, U., Roberts, J.M., 2016. The effect of flow speed and food size on the
684 capture efficiency and feeding behaviour of the cold-water coral Lophelia pertusa. Journal of
685 Experimental Marine Biology and Ecology 481, 34-40, 10.1016/j.jembe.2016.04.002.

686 Purser, A., 2015. A Time Series Study of Lophelia pertusa and Reef Megafauna Responses to
687 Drill Cuttings Exposure on the Norwegian Margin. PLoS ONE 10, e0134076,
688 10.1371/journal.pone.0134076.

689 Purser, A., Larsson, A.I., Thomsen, L., van Oevelen, D., 2010. The influence of flow velocity
690 and food concentration on *Lophelia pertusa* (Scleractinia) zooplankton capture rates. Journal
691 of Experimental Marine Biology and Ecology 395, 55-62, 10.1016/j.jembe.2010.08.013.

692 Raddatz, J., Rüggeberg, A., Liebetrau, V., Foubert, A., Hathorne, E.C., Fietzke, J., Eisenhauer,
693 A., Dullo, W.-C., 2014. Environmental boundary conditions of cold-water coral mound growth
694 over the last 3 million years in the Porcupine Seabight, Northeast Atlantic. Deep Sea Research
695 Part II: Topical Studies in Oceanography 99, 227-236,
696 http://dx.doi.org/10.1016/j.dsr2.2013.06.009.

697 Robert, K., Huvenne, V.A.I., Georgiopoulou, A., Jones, D.O.B., Marsh, L., D. O. Carter, G.,
698 Chaumillon, L., 2017. New approaches to high-resolution mapping of marine vertical
699 structures. Scientific Reports 7, 9005, 10.1038/s41598-017-09382-z.

700 Robert, K., Jones, D.O.B., Roberts, J.M., Huvenne, V.A.I., 2016. Improving predictive
701 mapping of deep-water habitats: Considering multiple model outputs and ensemble techniques.
702 Deep Sea Research Part I: Oceanographic Research Papers 113, 80-89,
703 http://dx.doi.org/10.1016/j.dsr.2016.04.008.

704 Roberts, J.M., Long, D., Wilson, J.B., Mortensen, P.B., Gage, J.D., 2003. The cold-water coral
705 Lophelia pertusa (Scleractinia) and enigmatic seabed mounds along the north-east Atlantic
706 margin: are they related? Marine Pollution Bulletin 46, 7-20, http://dx.doi.org/10.1016/S0025-
707 326X(02)00259-X.

708 Roberts, J.M., Wheeler, A.J., Cairns, S., Freiwald, A., 2009. Cold-water corals: the biology
709 and geology of deep-sea coral habitats. Cambridge University Press,
710 http://dx.doi.org/10.1017/CBO9780511581588.003.

711 Roberts, J.M., Wheeler, A.J., Freiwald, A., 2006. Reefs of the Deep: The Biology and Geology
712 of Cold-Water Coral Ecosystems. Science 312, 543-547,
713 http://dx.doi.org/10.1126/science.1119861.

714 Rüggeberg, A., Dullo, W.-C., Dorschel, B., Hebbeln, D., 2007. Environmental changes and
715 growth history of a cold-water carbonate mound (Propeller Mound, Porcupine Seabight).
716 International Journal of Earth Sciences 96, 57-72.

717 Savini, A., Vertino, A., Marchese, F., Beuck, L., Freiwald, A., 2014. Mapping cold-water coral
718 habitats at different scales within the Northern Ionian Sea (Central Mediterranean): an
719 assessment of coral coverage and associated vulnerability. PLoS ONE 9, e87108,
720 10.1371/journal.pone.0087108.

721 Squires, D.F., 1964. Fossil coral thickets in Wairarapa, New Zealand. Journal Paleontol. 38,
722 904-915.

723 Thompson, S.K., 1987. Sample size for estimating multinomial proportions. The American
724 Statistician 41, 42-46, http://dx.doi.org/10.2307/2684318.

725 Van Rooij, D., 2004. An integrated study of Quaternary sedimentary processes on the eastern
726 slope of the Porcupine Seabight, SW of Ireland. Ghent University,
727 http://dx.doi.org/1854/10815.

728 Vertino, A., Savini, A., Rosso, A., Di Geronimo, I., Mastrototaro, F., Sanfilippo, R., Gay, G.,
729 Etiope, G., 2010. Benthic habitat characterization and distribution from two representative sites
730 of the deep-water SML Coral Province (Mediterranean). Deep-Sea Research Part Ii-Topical
731 Studies in Oceanography 57, 380-396, 10.1016/j.dsr2.2009.08.023.

732 Wheeler, A.J., Beck, T., Thiede, J., Klages, M., Grehan, A., Monteys, F.X., Polarstern ARK
733 XIX/3a Shipboard Party, 2005. Deep-water coral mounds on the Porcupine Bank, Irish margin:
734 preliminary results from Polarstern ARK-XIX/3a ROV cruise, in: Freiwald, A., Roberts, J.M.
735 (Eds.), Cold-water corals and Ecosystems. Springer-Verlag, Berlin, pp. 393-402,
736 http://dx.doi.org/10.1007/3-540-27673-4_19.

737 Wheeler, A.J., Beyer, A., Freiwald, A., de Haas, H., Huvenne, V.A.I., Kozachenko, M., Olu-
738 Le Roy, K., Opderbecke, J., 2007. Morphology and environment of cold-water coral carbonate
739 mounds on the NW European margin. International Journal of Earth Sciences 96, 37-56,
740 http://dx.doi.org/10.1007/s00531-006-0130-6.

741 Wheeler, A.J., Kozachenko, M., Beyer, A., Foubert, A.T.G., Huvenne, V.A.I., Klages, M.,
742 Masson, D.G., Olu-Le Roy, K., Thiede, J., 2005. Sedimentary processes and carbonate mounds
743 in the Belgica Mound province, Porcupine Seabight, NE Atlantic, in: Freiwald, A., Roberts,
744 J.M. (Eds.), Cold-water Corals and Ecosystems. Springer-Verlag, Berlin Heidelberg, pp. 533-
745 564, http://dx.doi.org/10.1007/3-540-27673-4_28.

746 Wheeler, A.J., Kozachenko, M., Henry, L.A., Foubert, A., de Haas, H., Huvenne, V.A.I.,
747 Masson, D.G., Olu, K., 2011. The Moira Mounds, small cold-water coral banks in the
748 Porcupine Seabight, NE Atlantic: Part A—an early stage growth phase for future coral
749 carbonate mounds? Marine Geology 282, 53-64, 10.1016/j.margeo.2010.08.006.

750 Wheeler, A.J., Kozachenko, M., Masson, D.G., Huvenne, V.A.I., 2008. Influence of benthic
751 sediment transport on cold-water coral bank morphology and growth: the example of the
752 Darwin Mounds, north-east Atlantic. Sedimentology 55, 1875-1887, 10.1111/j.1365-
753 3091.2008.00970.x.

754 Wheeler, A.J., shipboard party, 2011. Vents & Reefs deep-sea ecosystem study of the 45˚ North
755 MAR hydrothermal vent field and the cold-water coral Moira Mounds, Porcupine Seabight,
756 Cruise report, p. 160.

Wheeler, A.J., Stadnitskaia, A., 2011. Benthic Deep-Sea Carbonates. Developments in Sedimentology 63, 397-455, http://dx.doi.org/10.1016/B978-0-444-53000-4.00006-8.

White, M., 2007. Benthic dynamics at the carbonate mound regions of the Porcupine Sea Bight continental margin. International Journal of Earth Sciences 96, 1-9, http://dx.doi.org/10.1007/s00531-006-0099-1.

Wienberg, C., Beuck, L., Heidkamp, S., Hebbeln, D., Freiwald, A., Pfannkuche, O., Monteys, F.X., 2008. Franken Mound: facies and biocoenoses on a newly-discovered "carbonate mound" on the western Rockall Bank, NE Atlantic. Facies 54, 1-24, 10.1007/s10347-007-0118-0.

Wienberg, C., Hebbeln, D., Fink, H.G., Mienis, F., Dorschel, B., Vertino, A., López Correa, M., Freiwald, A., 2009. Scleractinian cold-water corals in the Gulf of Cádiz-first clues about their spatial and temporal distribution. Deep Sea Research Part I 56, 1873-1893, doi:10.1016/j.dsr.2009.05.016.

Wilson, J.B., 1979. "Patch" development of the deep-water coral *Lophelia pertusa* (L.) on the Rockall bank. Journal of the Marine Biological Association of the United Kingdom 59, 165-177, http://dx.doi.org/10.1017/S0025315400046257.

784 Figures

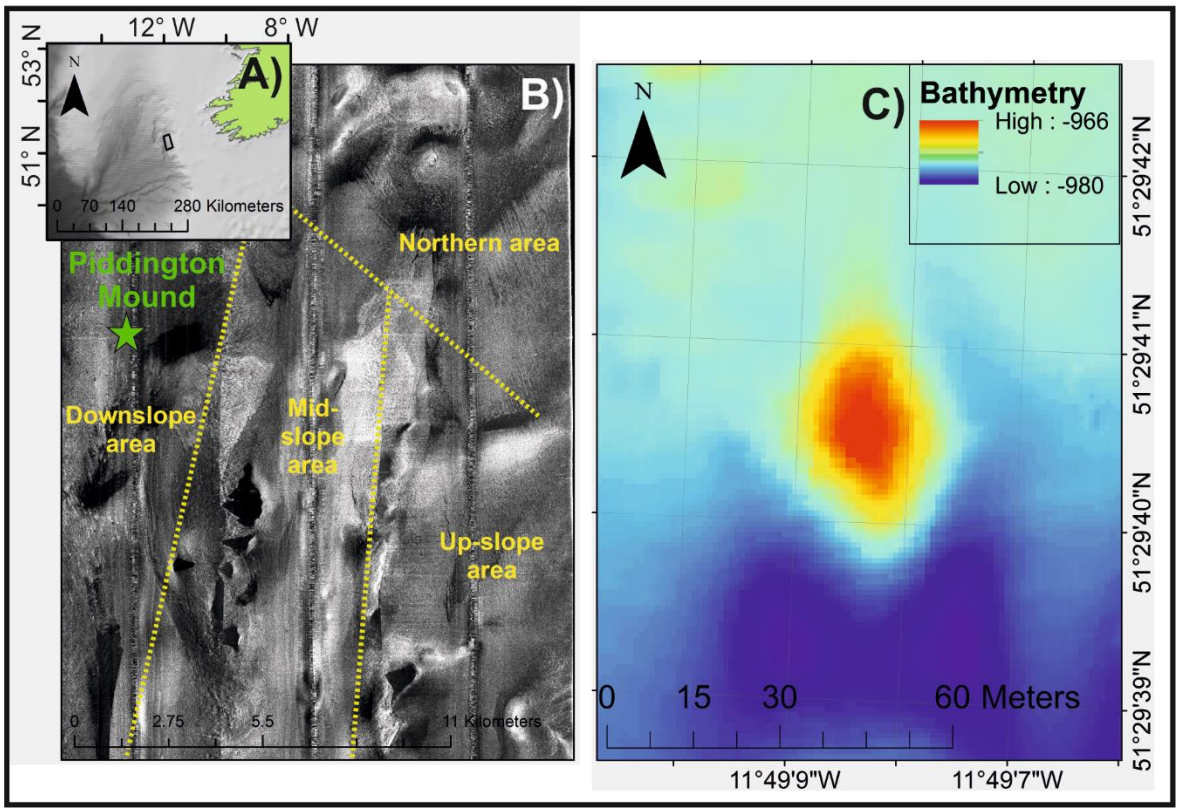

785

786 *Figure 1 Location map of study area*

787 A) Location of Belgica Mound Province (BMP) Special Area of Conservation (SAC) (black
788 box), offshore SW Ireland; B) 30 kHz TOBI side scan sonar imagery of the BMP SAC with
789 areas defined by Wheeler et al., (2011) in yellow and location of Piddington Mound indicated
790 by green star; C) Piddington Mound bathymetry (meters).

791

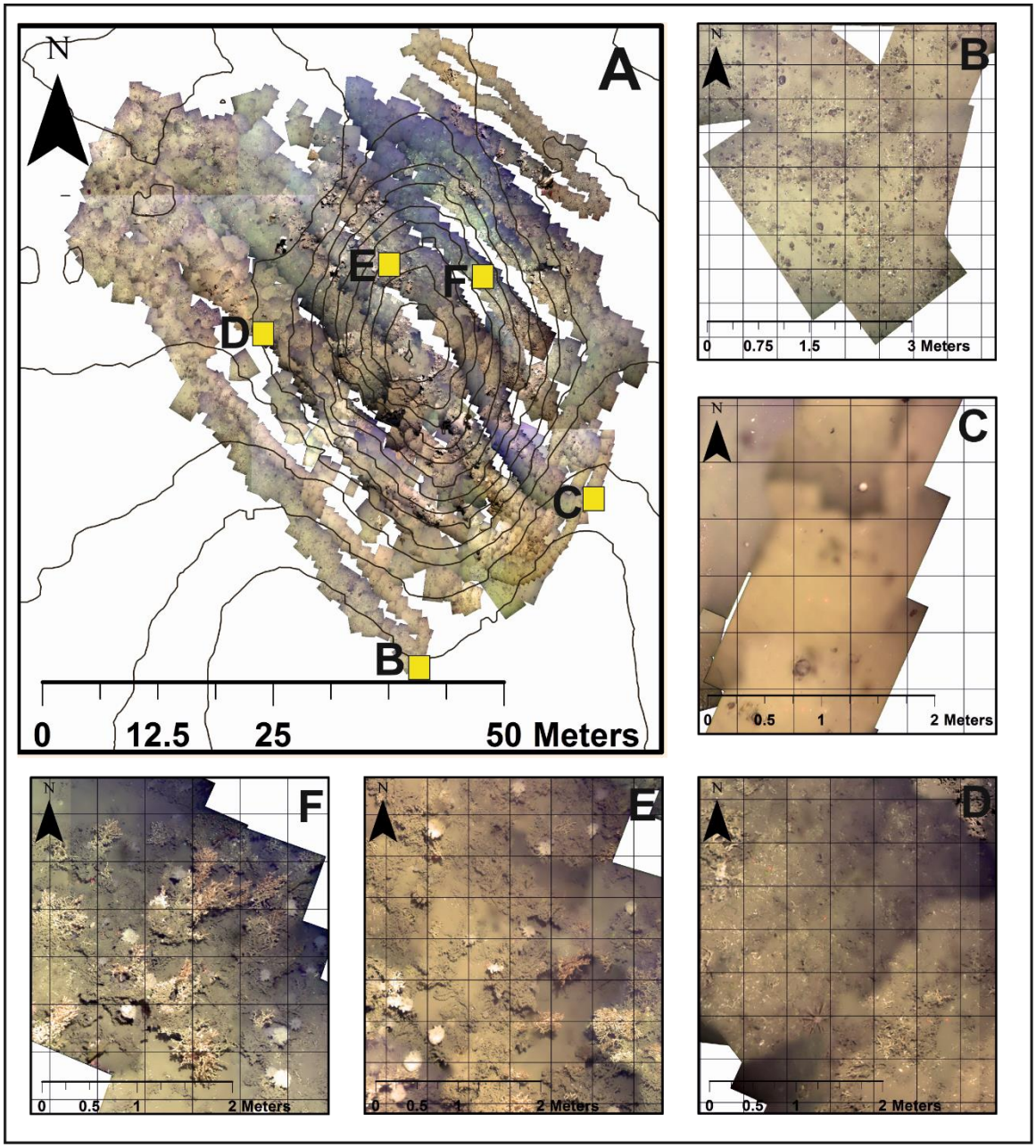

792

793 Figure 2 Map of the Piddington Mound video mosaic and examples of classes: A) mosaicked
794 area with 1 m contours superimposed, B) example of the "hemipelagic sediment with
795 dropstones" class, C) example of the "hemipelagic sediment" class, D) example of the "coral
796 rubble" class, E) example of the "dead coral framework" class, and F) example of the "live
797 coral framework" class.

798

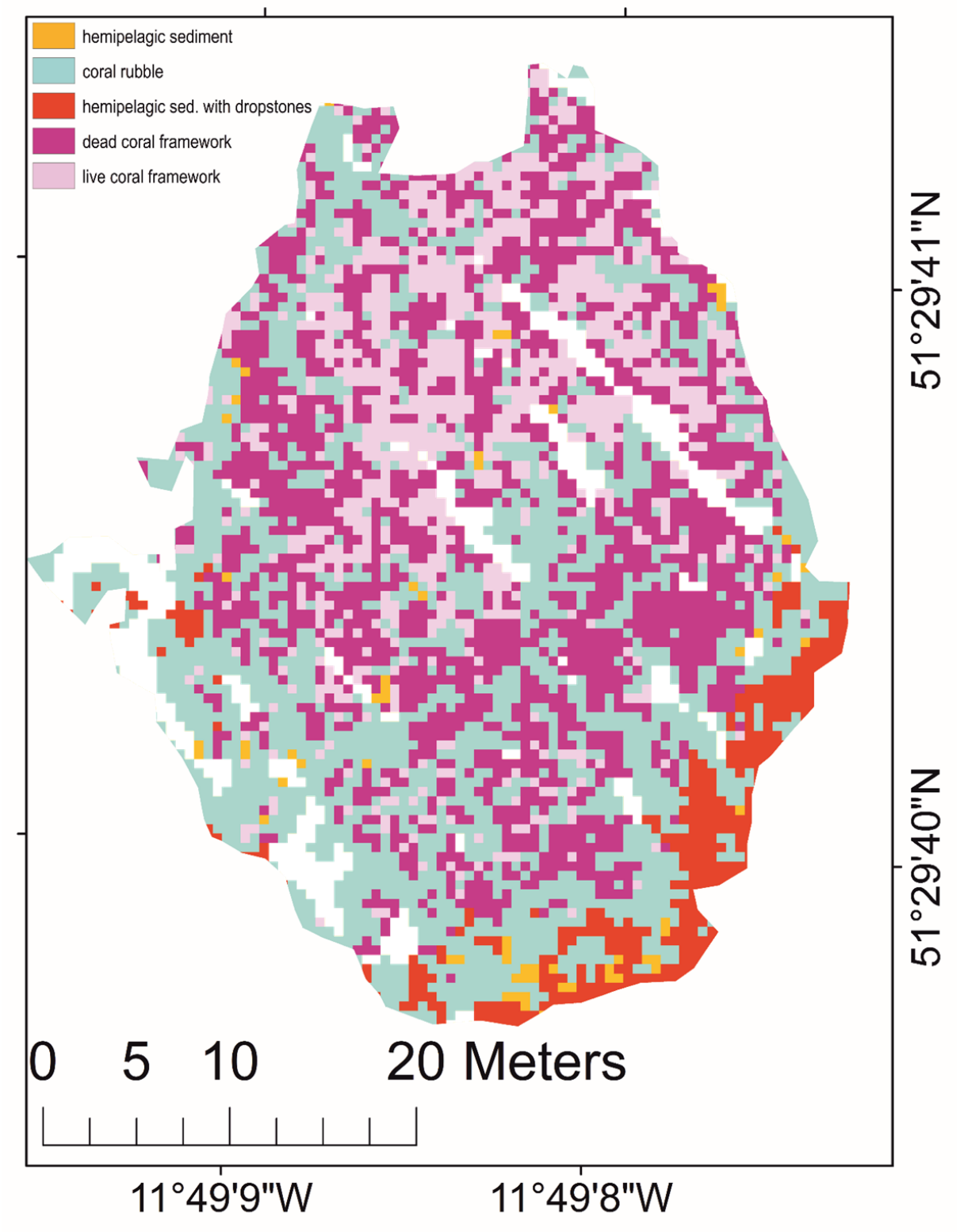

799

800 *Figure 3 Classified mosaic*

801 *Blue= coral rubble cells; red=sediment and dropstone cells; orange= hemipelagic sediment*
802 *cells; magenta=dead coral framework cells; and pink=live coral framework cells.*

803

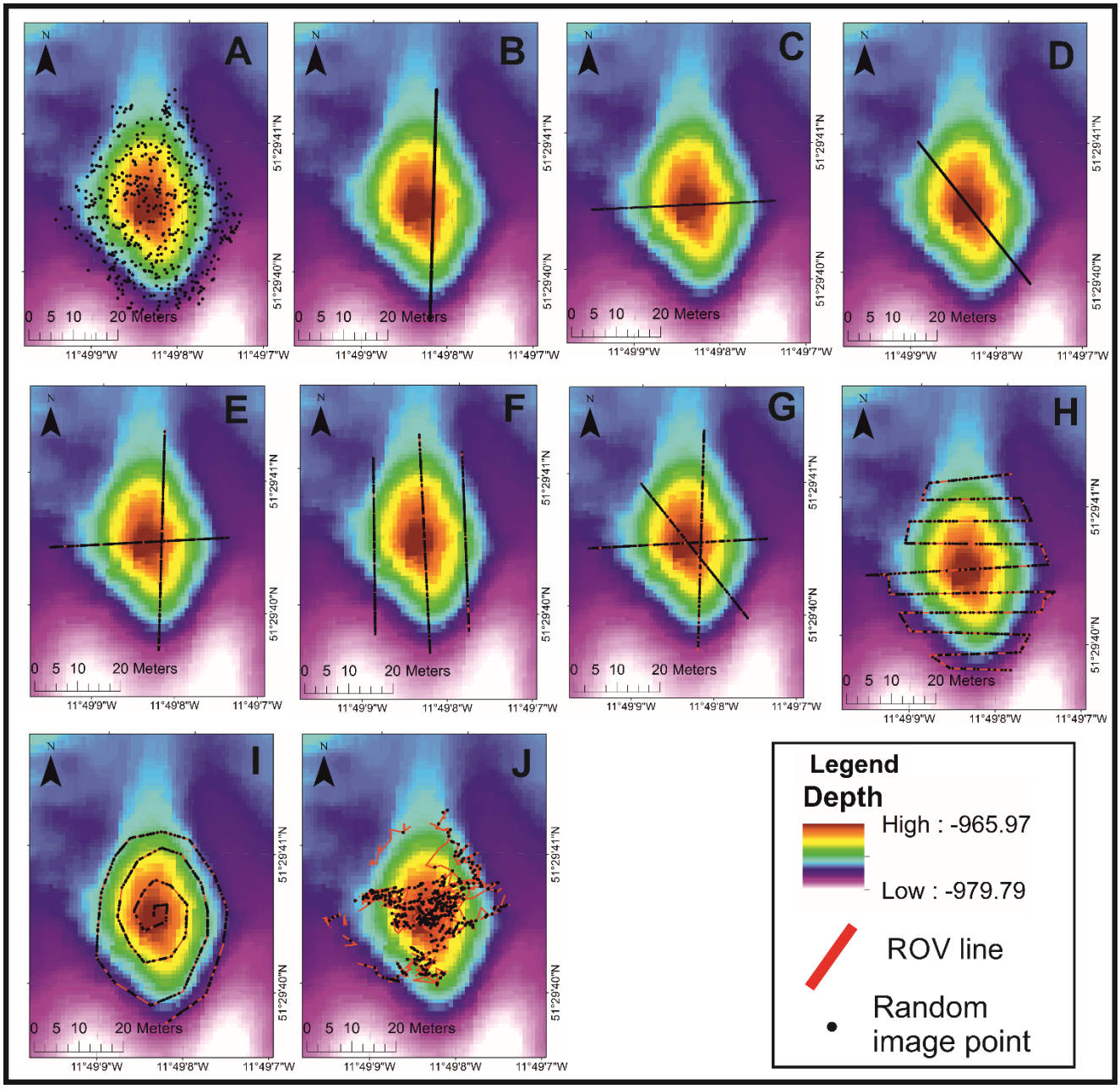

804

805 *Figure 4 Video-survey designs facilitating the collection of X=510 random image points*
806 *along the survey lines*

807 *A) random points (SD1), B) south-north transect (SD2), C) east-west transect (SD3), D)*
808 *northwest-southeast diagonal transect (SD4), E) 2 lines (SD5), F) 3 straight, parallel line*
809 *grid (SD6), G) 3 summit-crossing lines (SD7), H) horizontal grid (SD8), I) spiral (SD9)*
810 *and J) an actual survey transect from a mound reconnaissance dive (SD10).*

811

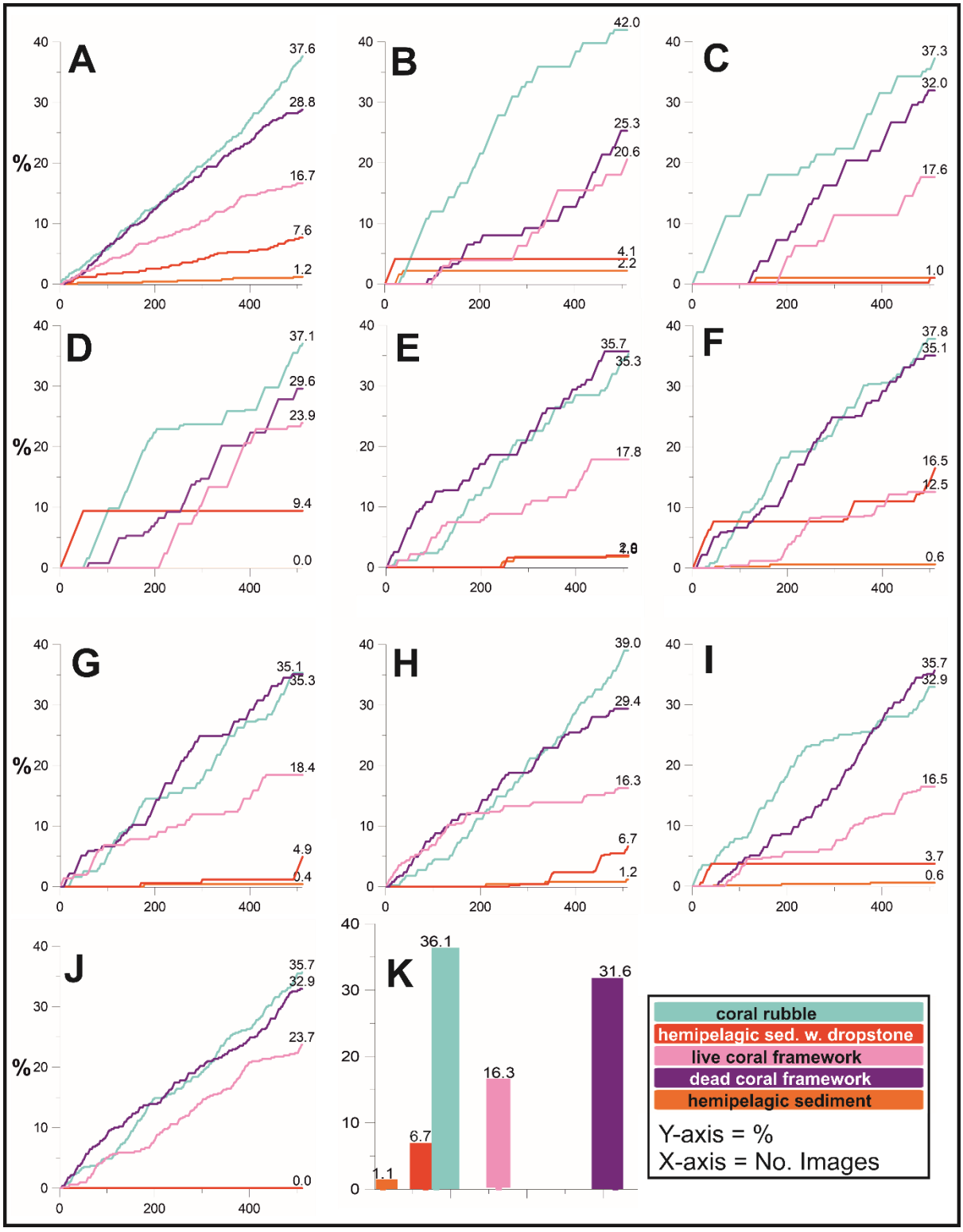

812

813 *Figure 5* survey design results presented as facies sampling curves. *A) random points (SD1),*
814 *B) south-north transect (SD2), C) east-west transect (SD3), D) northwest-southeast diagonal*
815 *transect (SD4), E) 2 lines (SD5), F) 3 straight, parallel line grid (SD6), G) 3 summit-crossing*
816 *lines (SD7), H) horizontal grid (SD8), I) spiral (SD9), J) an actual survey transect from a*
817 *mound reconnaissance dive (SD10) and K) single axis bar chart showing the total proportion*
818 *of observed facies across the Piddington Mound. A) to J) y-axis=% percentage of facies, x-*
819 *axis= number of images, K) y-axis=%*

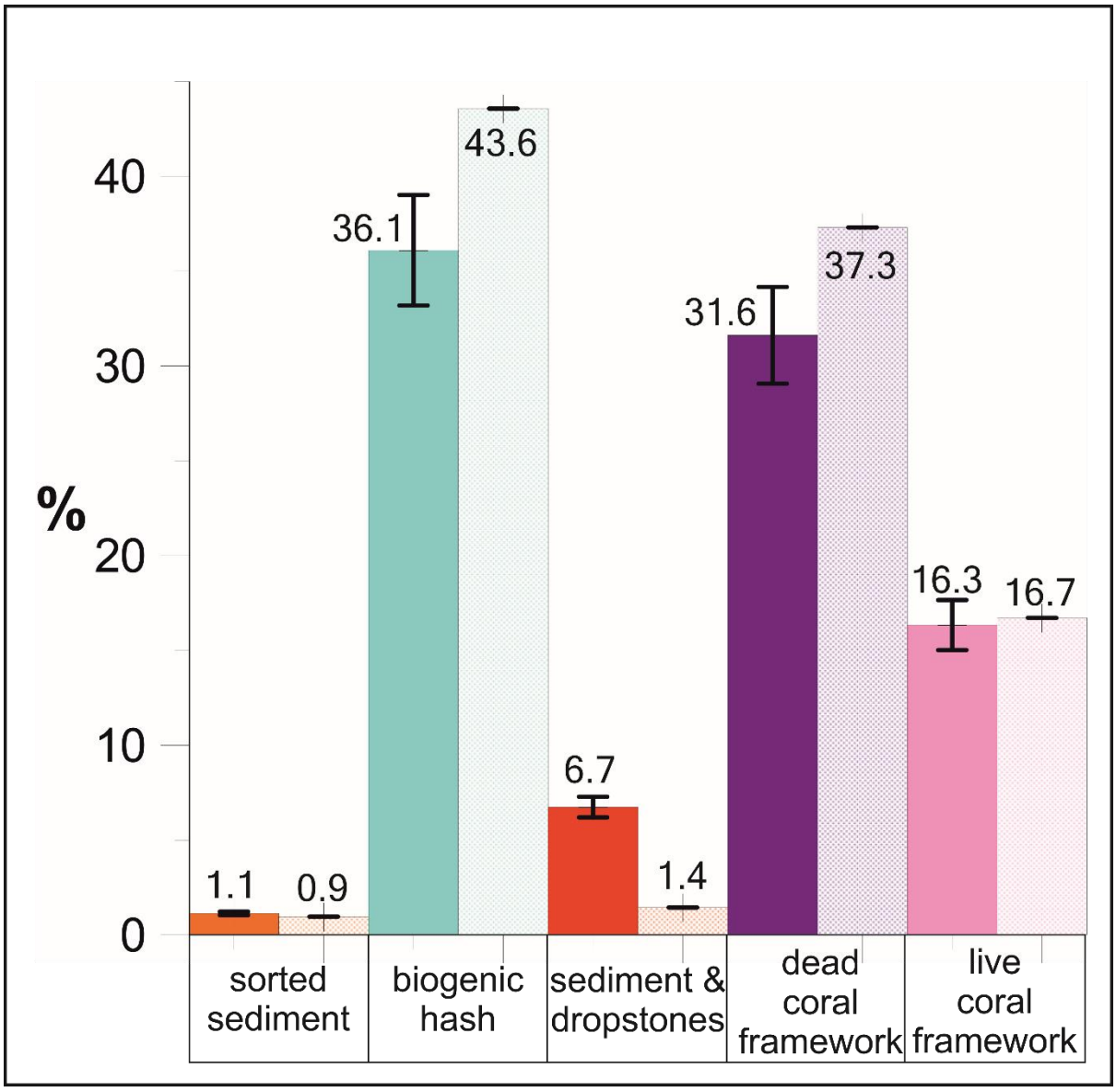

Figure 6 Graph comparing T1 and T4 facies.

T1 Piddington Mound cell-type proportions in checker fill. T4 Piddington Mound cell-type proportions in solid fill.

alpha (α)	(d^2 * n)	m	*X* = (n if d = 0.05)
0.5	0.44129	4	177
0.4	0.50729	4	203
0.3	0.60123	3	241
0.2	0.74739	3	299
0.1	1.00635	3	403
0.05	1.27359	3	510
0.025	1.55963	2	624
0.02	1.65872	2	664
0.01	1.96986	2	788
0.005	2.28514	2	915
0.001	3.02892	2	1212
0.0005	3.3353	2	1342
0.0001	4.11209	2	1645

827

828 *Table 1 Minimum sample size estimation table after Thompson (1987)*

829 *Alpha values (α) represents the significance level which can be used to calculate the confidence*
830 *level (e.g. an alpha of 0.05 gives a confidence level of 95%), d is the margin of error, n is the*
831 *sample size, m is the minimum number of categories required (see Thompson (1987) for further*
832 *details on m), X is sample size.*

833

Class	Description	Typical Environment
hemipelagic sediment	cell dominated (>90 % cell coverage) by hemipelagic sediment i.e. sand or mud with no recognisable bioclasts or dropstones	no dropstones nor deposition of biogenic material. Potentially deposition of a sorted sediment under the influence of benthic currents.
coral rubble	cell dominated (>50 % cell coverage) by recognisable biogenic material (i.e. coral rubble, shell fragments) and sediment	deposition of mound-derived material
hemipelagic sediment with dropstones	cell dominated (>50 % cell coverage) by dropstones and sediment (sand or mud)	erosion, non-deposition or non-coral growth since the deposition of the dropstones
dead coral framework	cell dominated (>50 % cell coverage) by coral framework which has no identifiable living parts	coral no longer grows
live coral framework	cell dominated (>50 % cell coverage) by coral framework with identifiable living parts	coral growth

834 *Table 2 Facies description*

835

Class	T1_%	T4_%	Δ_%
hemipelagic sediment	1.14 (±0.09)	0.96	-0.18
coral rubble	36.1 (±3.14)	43.57	7.47
hemipelagic sediment with dropstones	6.74 (±0.58)	1.45	-5.29
dead coral framework	31.61 (±2.75)	37.3	5.69
live coral framework	16.38 (±1.42)	16.72	0.34
no data	8	0	
Sum of classified cells	100.0	100.0	

836

837 *Table 3 Comparison of T1 Piddington Mound cell-type proportions (T1_%) with T4*
838 *Piddington Mound proportions (T4_%).*

839 *The Δ_% column represents the percentage change between T1 and T4. All values are rounded*
840 *up to the nearest two decimal places. Error margins are proportionally distributed from "no*
841 *data" values.*

842